IET Microwaves, Antennas & Propagation

Research Article

Beam-scanning leaky-wave antenna based on CRLH-metamaterial for millimetre-wave applications

ISSN 1751-8725
Received on 23rd March 2018
Revised 17th December 2018
Accepted on 4th March 2019
E-First on 26th March 2019
doi: 10.1049/iet-map.2018.5101
www.ietdl.org

Mohammad Alibakhshikenari[1] ✉, Bal S. Virdee[2], Mohsen Khalily[3], Panchamkumar Shukla[2], Chan H. See[4,5], Raed Abd-Alhameed[6,7], Francisco Falcone[8], Ernesto Limiti[1]

[1]*Electronic Engineering Department, University of Rome "Tor Vergata", Via del politecnico 00133, Rome, Italy*
[2]*London Metropolitan University, Center for Communications Technology & Mathematics, School of Computing & Digital Media, London N7 8DB, UK*
[3]*Institute for Communication Systems, Home of 5G Innovation Centre (5GIC), University of Surrey, Guildford, GU2 7XH, UK*
[4]*School of Engineering and the Built Environment, Edinburgh Napier University, 10 Colinton Road, Edinburgh, EH10 5DT, UK*
[5]*School of Engineering, University of Bolton, Deane Road, Bolton, BL3 5AB, UK*
[6]*School of Electrical Engineering & Computer Science, University of Bradford, Bradford, BD7 1DP, UK*
[7]*Department of Communication and Informatics Engineering, Basra University College of Science and Technology, Basra 61004, Iraq*
[8]*Electric and Electronic Engineering Department, Universidad Pública de Navarra, Spain*
✉ *E-mail: alibakhshikenari@ing.uniroma2.it*

Abstract: This paper presents empirical results of an innovative beam-scanning leaky-wave antenna (LWA), which enables scanning over a wide angle from − 35° to + 34.5° between 57 and 62 GHz, with broadside radiation centred at 60 GHz. The proposed LWA design is based on composite right/left-handed transmission-line (CRLH-TL) concept. The single-layer antenna structure includes a matrix of 3 × 9 square slots that is printed on top of the dielectric substrate; and printed on the bottom ground-plane are Π- and T-shaped slots that enhance the impedance bandwidth and radiation properties of the antenna. The proposed antenna structure exhibits metamaterial property. The slot matrix provides beam scanning as a function of frequency. Physical and electrical size of the antenna is 18.7 × 6 × 1.6 mm^3 and $3.43\lambda_0 \times 1.1\lambda_0 \times 0.29\lambda_0$, respectively, where λ_0 is free space wavelength at 55 GHz. The antenna has a measured impedance bandwidth of 10 GHz (55–65 GHz) or fractional bandwidth of 16.7%. Its optimum gain and efficiency are 7.8 dBi and 84.2% at 62 GHz.

1 Introduction

Lower end of the EM spectrum is highly congested as wireless networks operating in the unlicensed ISM band at 2.45 and 5 GHz that are extensively used for transmitting large amounts of data including high-resolution images and high-definition videos. In fact, the mobile data traffic is growing exponentially which cannot be sustained much longer over the existing wireless infrastructure hence the inevitable need for 60 GHz band will enable multi-gigabit per second transmission with low latency.

The 60 GHz band offers an enormous unlicensed bandwidth and its exploitation will deliver significant benefits for existing wireless communications networks and will enable a diverse range of new wireless products and services envisioned for Internet of Things (IoT) and fifth-generation (5G) mobile systems. This means transmission of uncompressed video, which is almost an 'impossible mission' in the current microwave bands, has become possible. However, propagation of millimetre waves can easily be impeded by physical objects like buildings and trees, which can, therefore, degrade the system performance. This can be avoided by using beam steering antennas. In radar systems, phase shifters are typically used to control the direction of the main beam; however, these components are lossy and expensive at millimetre-wave. An efficient and economical way to accomplish beam steering is by using leaky-wave antennas (LWA), which have been investigated extensively for applications including imaging [1] and automotive radar [1, 2]. LWAs are guiding structures on which a travelling wave propagates but leaks out of a radiating aperture [3]. They are a class of travelling wave antennas where the aperture extends over several wavelengths; the longer the aperture, the narrower is the radiation beam. LWAs present several advantages that include (i) simplicity of design since no feeding network is needed and (ii) capability of frequency scanning of the radiating pattern. LWA based on composite right/left-handed (CRLH) was first demonstrated in [4] and has been shown to provide beam scanning from backfire to endfire [5–7]. Such antennas include vias and/or interdigital structures to realise CRLH-TLs, which introduces design and manufacturing complexity to the antenna that has an impact on cost. Hence, despite considerable progress being made in the development of LWAs, there is still room for innovation and improvement in terms of the following parameters: (i) wider beam-scanning; (ii) reduction in reflection-coefficient and side-lobe level (SLL); (iii) greater directivity, radiation efficiency, and gain; (iv) smaller physical footprint; and (v) reduced design/manufacturing complexity.

Here, a novel wide-area beam-scanning LWA design is presented for millimetre-wave applications. The antenna design is based on conventional planar microstrip integrated circuit technology and the concept of CRLH transmission-line metamaterial methodologies [8, 9]. The resulting LWA has a small physical footprint and relatively large beam-scanning from −35° to + 34.5° over its operating frequency of 55–65 GHz. The proposed LWA is compact with dimensions of 18.7 × 6 × 1.6 mm^3. Gain and radiation efficiency variation of the LWA over its operating frequency range are 4.3–7.8 dBi and 55.4–84.2%, respectively.

2 CRLH-TL leaky-wave antenna

2.1 Fundamental metamaterial structure

Left-handed transmission line (LH-TL) can be realised by cascading together unit cells such as the one shown in Fig. 1*a* comprised of a T-shape electrical circuit constituted from series capacitors and shunted inductor. This is a dual circuit of a conventional transmission line, shown in Fig. 1*b*. In reality, it is not possible to realise a purely LH-TL as the parasitic effects of the

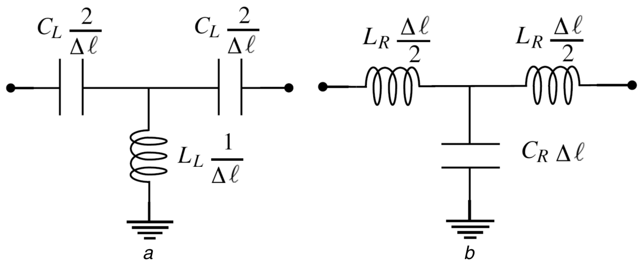

Fig. 1. *Equivalent circuits of a short transmission line ($\beta\Delta l \ll 1$)*
(a) Left-handed *LC* equivalent circuit and ***(b)*** Right-handed *LC* equivalent circuit

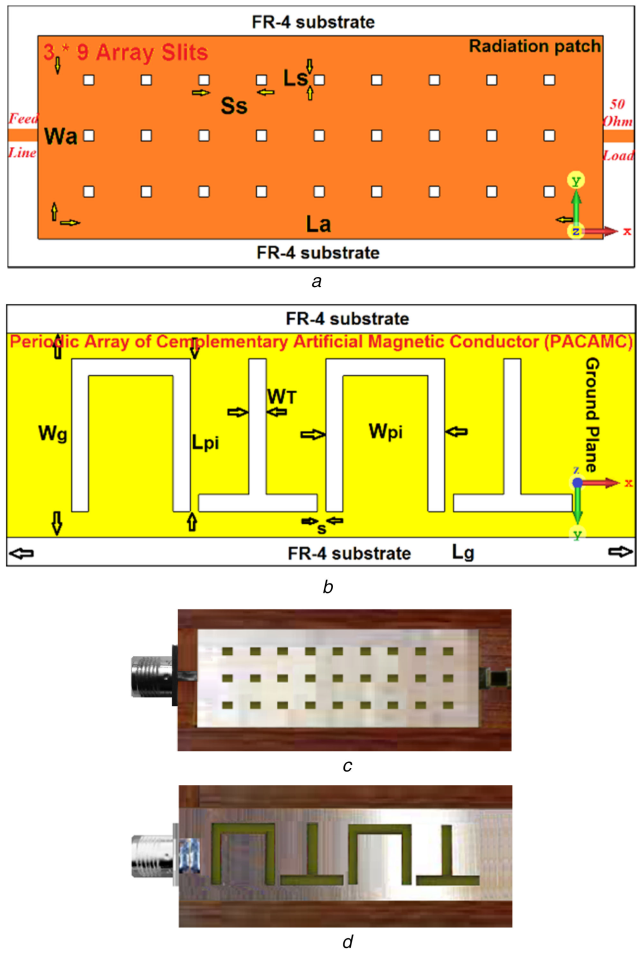

Fig. 2. *The proposed leaky-wave antenna configuration and the fabricated prototype*
(a) Top view of the leaky-wave antenna, ***(b)***Bottom view of the leaky-wave antenna, ***(c)*** Top view of the LWA prototype, ***(d)*** Bottom view of the LWA prototype

capacitors and the inductor in Fig. 1*a* results in a combined behaviour resulting in the so-called artificial CRLH transmission lines [10, 11].

A pure LH-TL can support backward waves [12]. The propagation constant of the LH-TL is $\beta_L(\omega) = -1/\omega\sqrt{L_L C_L}$, where L_L and C_L are the inductance and capacitance per unit length, respectively. Its equivalent permittivity and permeability are both less than zero. Hence, the equivalent refraction index is less than zero as well, which confirms its left-handed nature. With this ideal structure, it is possible for radiation to backfire. However, in the case of a conventional LWA, i.e. right-handed transmission lines, the antenna radiates in the forward directions that is limited by the nature of conventional transmission lines. In reality, the LH-TL structure is a CRLH transmission line (CRLH-TL). The propagation constant is, therefore, $\beta_C = \omega\sqrt{L_R C_R} - 1/\omega\sqrt{L_L C_L}$, where L_R and C_R are the series inductance and shunt capacitance per unit length, respectively [13]. A CRLH-TL is dominant LH mode while $f < f_0$, RH mode while $f > f_0$, and with infinite

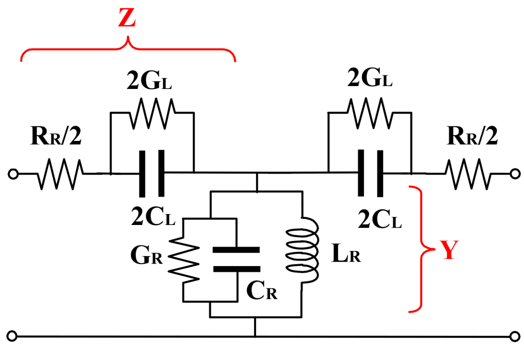

Fig. 3. *Equivalent circuit model of the unit-cell constituting the LWA*

wavelength while $f = f_0$ [14]. β_C varies from negative to positive with the increase of frequency. This property is exploited here to realise a LWA based to enable the antenna to radiate from backfire to endfire direction [15].

2.2 B Proposed antenna structure

The proposed LWA comprises 3 × 9 array of square slots etched on the top-side of the dielectric substrate board and the bottom-side of the substrate is the ground-plane, which is loaded with Π-shaped and T-shaped slots, as shown in Fig. 2. The antenna is excited from one end and is terminated with a matched 50Ω load on the other end. The 3 × 9 array was optimised to achieve beam-steering from an angle of −35° to + 34.5°. By loading the ground-plane with Π- and T-shaped slots results in enhancement of the antenna's effective aperture. This modification to the antenna structure improved its impedance bandwidth and radiation properties, i.e. gain and efficiency, without increasing its physical dimensions as will be shown later. This is because the ground-plane slots essentially form a partially reflective surface that increases the value of the attenuation constant of the leaky-mode causing radiation. The radiated power through the slots is determined by the interference of waves partially transmitted through the partially reflected surface. The proposed LWA was designed and manufactured on a standard commercially available printed circuit board dielectric substrate FR-4 having dielectric constant of $\varepsilon_r = 4.3$, loss-tangent $\tan\delta = 0.025$, and thickness of $h = 1.6$ mm.

Simplified equivalent circuit model of the unit cell constituting the antenna shown in Fig. 3 was deduced from [16] where the square slots in the top layer essentially are capacitive in nature, and the slots in the ground-plane act as capacitive iris. This circuit approximates to a typical CRLH structure.

The antenna in Fig. 2 can be approximated to a slotted waveguide. The signal launched from the connector travels towards the load in the *x*-direction. The wave leaks from the slotted structure gradually. This causes the radiation from the antenna to have a narrow beam which is highly directive. EM-fields in the upper space leaked from the slotted structure in the *xz*-direction assuming the general time dependence as $e^{j\omega t}$ are defined by:

$$H_y = H_o e^{-jk_x x - jk_z z} \tag{1a}$$

$$E_x = \frac{K_z}{\omega\varepsilon_o} H_o e^{-jk_x x - jk_z z} \tag{1b}$$

$$E_z = \frac{-K_x}{\omega\varepsilon_o} H_o e^{-jk_x x - jk_z z} \tag{1c}$$

For lossless media, $k_x = \beta_x$ is the propagating constant along the $+x$ direction, and $k_z = \alpha_z$ is the propagating constant along the $+z$ direction (α_z is a positive real number). Phase constant is defined as $\beta_x = \omega/v_p$, where v_p is phase velocity. The relationship between the k_x and k_z can be written as [4]

$$k_x = \sqrt{k_o^2 - k_z^2} \tag{2}$$

where k_0 is the wavenumber in free space. When the wave velocity is faster than the velocity of light (or $\beta_x < k_o$), the beam scanning angle θ in the xz-plane can be determined by

$$\sin\theta = \beta_x / k_o \tag{3}$$

At the resonance frequency, the magnitudes of C_L, C_R, and L_R of the circuit in Fig. 3 were determined from the dispersion graph of the proposed CRLH-TL structure. This was obtained by applying the boundary conditions related to the Bloch–Floquet theorem, i.e.:

$$\varnothing(\omega) = \beta(\omega)p = \cos^{-1}\left(1 + \frac{ZY}{2}\right) \tag{4}$$

$$Z(\omega) = \mathrm{j}\left(\omega L_\mathrm{R} - \frac{1}{\omega C_\mathrm{L}}\right) \tag{5}$$

$$Y(\omega) = \mathrm{j}\left(\omega C_\mathrm{R} - \frac{1}{\omega L_\mathrm{L}}\right) \xrightarrow{\mathrm{SCRLH-TL\ without\ L_L}} Y(\omega) = \mathrm{j}(\omega C_\mathrm{R}) \tag{6}$$

where p is the periodicity of the ground-plane slots [4]. The unit-cell depicted in Fig. 3 is characterised by impedance Z and admittance Y. The series right-hand (RH) inductance is denoted by L_R, and the shunt RH capacitance by C_R. The phase relation is obtained by substituting (5) and (6) into (4), i.e.

$$\varnothing(\omega) = \cos^{-1}\left\{1 - \left[\frac{1}{2}\frac{C_\mathrm{R}}{C_\mathrm{L}}(\omega^2 C_\mathrm{L} L_\mathrm{R} - 1)\right]\right\} \tag{7}$$

Fig. 4 depicts the phase of the LWA based on the proposed CRLH-TL as determined by HFSS™ and using (7). This shows the leaky-wave range of operation lies between the two air-lines from 55 to 65 GHz. In this region, the phase of the CRLH-TL is less than that of the free-space k_o, and, therefore, the wave progressively leaks out as it travels along the line. From the dispersion curve, the left-handed property is observed from 55 to 58 GHz as the phase velocity is antiparallel to the group velocity. From 58 to 65 GHz, on the other hand, the right-handed property takes place where the phase velocity is parallel to the group velocity. Fig. 4 also shows the normalised attenuation constant which is almost flat across 55–65 GHz and determines the radiation efficiency and beamwidth.

Electrical size of the CRLH-TL structure was reduced by increasing C_L, $L_\mathrm{R,}$ and C_R. This was accomplished by modifying the dimensions of the structure. This was done by using the optimisation technique available within HFSS™ which led to the final dimensions of the antenna given in Table 1. Magnitudes of the unit cell LC elements given in Table 2 were retrieved by approximate analytical expressions.

Broadside radiation from a unidirectional LWA is generally a challenge. The technique employed here to close the stop band existing around broadside frequency and to optimise radiation based on [17]. This was achieved by using unit cells comprising series and shunt resonators. When the resonant frequencies of the series and shunt resonators are made equal, a closed stop band is achieved. LWA's simulated and measured reflection coefficient response when loaded with and without ground-plane slots are shown in Fig. 5. When the slots are applied to the antenna, its impedance bandwidth increases due to increase in the number of resonance responses.

LWA without ground-plane slots have an impedance bandwidth of 8.4 GHz for S_{11}<−10 dB from 56.2 to 64.6 GHz, which corresponds to a fractional bandwidth (FBW) of 13.9%. In addition, antenna resonates at one frequency of 59.45 GHz. By loading the antenna with slots on its ground-plane the antenna's impedance bandwidth increases to 10.9 GHz in simulation case from 54.5 to 65.4 GHz with FBW of 18.18%. The measured impedance bandwidth is 10 from 55 to 65 GHz with FBW of 16.66%. In this case, the antenna resonates at three resonance frequencies of f_{r_1} = 57 GHz, f_{r_2} = 60 GHz, and f_{r_3} = 62 GHz that are exhibited in Fig. 5.

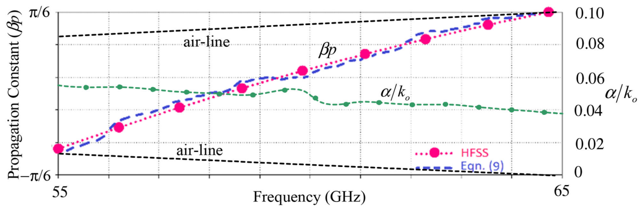

Fig. 4. *Phase & attenuation graph of the LWA in Fig. 2*

Table 1 Antenna structural dimensions (units in millimetres)

L_a	W_a	L_g	W_g	L_s	S_s	L_{pi}	W_{pi}	W_T	S
13.9	3.7	18.7	6.0	0.3	1.4	4.5	3.5	0.5	0.25

Table 2 Magnitudes of the unit cell LC values

Parameters	C_L, pF	C_R, pF	L_R, nH
Slot array	0.5	4.9	6.2
PACAMC-MTM array	8.7	3.7	4.8

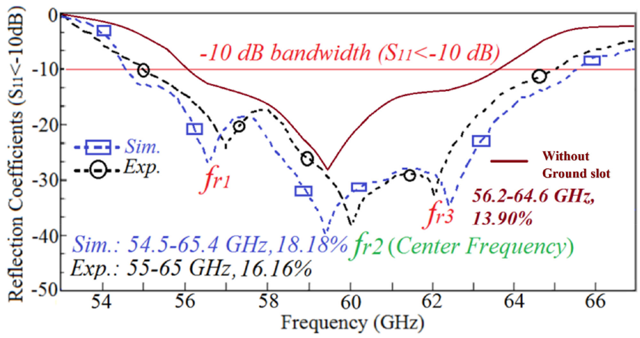

Fig. 5. *Reflection coefficient response of the proposed LWA with and without ground-plane slots. Dashed lines represent the case with slots*

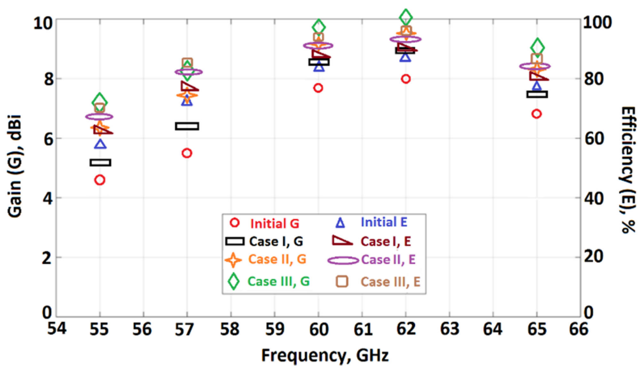

Fig. 6. *Gain (G) and efficiency (E) frequency response of the proposed LWA as a function of antenna length. In Case I, the initial antenna length is increased by 1.7 mm; In Case II, the antenna length is increased by 3.4 mm; and in Case III, the antenna length is increased by 5.1 mm*

Parameter study on how the antenna length affects gain and efficiency performance is shown in Fig. 6. In Case I, the antenna length ($Ls + Ss$) is 1.7 mm; in Case II, the antenna length is 3.4 mm; and in Case III, the antenna length is 5.1 mm. Results reveal that both the gain and efficiency are enhanced with increase in antenna length. This is because by increasing the antenna length, the effective aperture of the antenna is correspondingly increased [18]. Optimum gain and efficiency are observed at 62 GHz, where the gain has been increased from 8 dBi to 10 dBi, and the efficiency from 87.9 to 95%.

Gain of the antenna was measured using a standard anechoic-chamber. The set-up consisted of a transmitting horn antenna located at the focal-point of the reflector, which converted the spherical waves to plane waves towards the antenna under test. Standard comparative method was used to determine the antenna

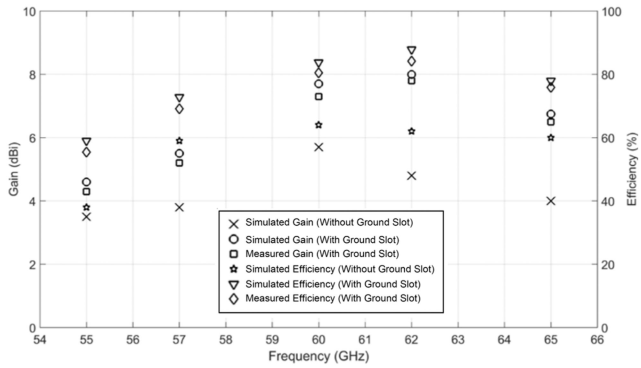

Fig. 7. *Gain and radiation efficiency response of the proposed LWA when it's unloaded and loaded with ground-plane slots*

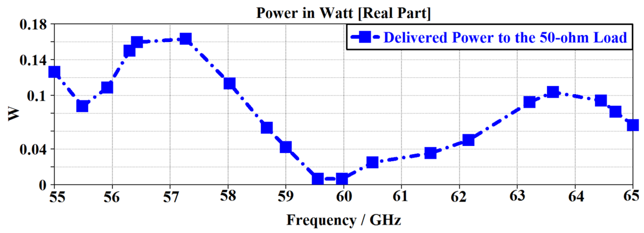

Fig. 8. *Delivered power to 50 Ω load*

gain. The radiation efficiency was calculated by taking the ratio of the gain to the directivity (i.e. $\eta = G/D$). Directivity was determined by measuring the half-power beamwidth of the antenna in the H-plane ($HPBW_H$) and in the E-plane ($HPBW_E$). Directivity was then calculated using the equation $D = 10\log_{10}[4\pi/(HPBW_H \times HPBW_E)]$ [19].

Simulated and measured gain and radiation efficiency of the antenna at several spot frequencies over its operational frequency are plotted in Fig. 7. It is evident that over this frequency range, the antenna's simulated gain varies from 4.6 to 8.0 dBi, and its measured gain varies from 4.3 to 7.8 dBi. The simulated efficiency varies from 59 to 87.9%, and its measured efficiency varies from 55.4 to 84.2%. These results show good agreement between the simulation and measurement. Maximum measured gain and radiation efficiency of 7.8 dBi and 84.2%, respectively, are obtained at second resonance frequency of 62 GHz. Minimum gain and radiation efficiency of 4.3 dBi and 55.4%, respectively, are obtained at 55 GHz.

Fig. 8 shows how the power delivered to the 50 Ω load varies over 55 to 65 GHz when the LWA is excited at its input with 0.178 W. The measurements show the power over the load varies between 0.01 and 0.16 W and is minimal at around 60 GHz.

Simulated and measured radiation patterns of the antenna at 55, 60, and 65 GHz are plotted in Fig. 9. These results show that the antenna is capable of scanning over an angle −35° to + 34.5° with frequency variation from 55 to 65 GHz. Backward, broadside and forward radiation occur at 55, 60, and 65 GHz, respectively. Fig. 9 also shows the simulated backward radiation in the E-plane with no slots in the ground-plane. The results show the slots reduce the back radiation owing to the suppression of surface wave diffraction from the edges of the conventional ground-plane. These results confirm the metamaterial property of the proposed LWA. Continuous beam-scanning from backfire to end-fire directions is, therefore, achievable. The measured 3 dB-beamwidth at 55, 60, and 65 GHz are 24°, 8.4°, and 20°, respectively. Considering the electrical size of the Π- and T-shaped slots on the bottom side of the substrate, it is, therefore, not surprising that radiation from the bottom is considerably attenuated as is evident in Fig. 9. This is because the resonant frequency of the slots is at much lower frequency than the operating range of the LWA. The results also demonstrate that the proposed LWA design with capability of beam-steering from − 35° to + 34.5° can be used for various applications especially for short-range radar, airport body scanners, and remote sensing in cars.

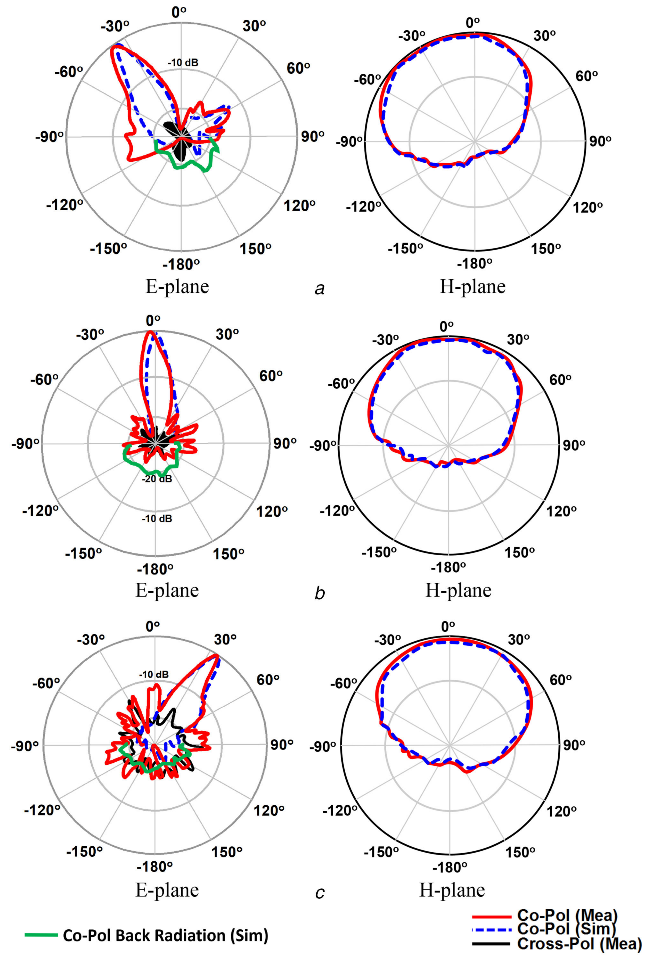

Fig. 9. *Simulated and measured E-plane (xz-plane) and H-plane (yz-plane) backward to forward radiation patterns of the proposed beam-steering antenna at*
(a) 55 GHz, ***(b)*** 60 GHz, and ***(c)*** 65 GHz

The proposed antenna is compared with other recent LWAs in Table 3. Compared to other millimetre-wave LWAs operating in a similar frequency range [20, 22], the present work exhibits a larger scan angle and larger fractional bandwidth but has a lower gain performance due to its shorter aperture length. The efficiency of LWA in [20, 22] is unspecified. The high radiation efficiency of the proposed antenna of 84.2% at 62 GHz is attributed to the excellent impedance matching (see Fig. 5), where the reflection coefficient is around −30 dB at 62 GHz. The excellent impedance matching here has achieved even though we used a cheap dielectric substrate (FR-4) with loss-tangent of tan δ = 0.025 at the millimetre waves [23, 24].

3 Conclusions

A novel LWA design has been demonstrated in practice. The planar antenna is designed using CRLH transmission lines metamaterial methodologies. The proposed antenna is compact with dimensions of $18.7 \times 6 \times 1.6\ mm^3$ and offers wide beam-scanning over an angle of −35° to + 34.5° over its operating frequency from 55 to 65 GHz. The measured gain and radiation efficiency variation of the LWA over this frequency range are 4.3–7.8 dBi and 55.4–84.2%, respectively. The antenna is low profile, lightweight, and inexpensive to fabricate in mass production.

4 Acknowledgments

This work was partially supported by innovation programme under grant agreement H2020-MSCA-ITN-2016 SECRET-722424 and financial support from the UK Engineering and Physical Sciences Research Council (EPSRC) under grant EP/E022936/1.

Table 3 Comparison of the proposed LWA with recently reported CRLH LWAs

Ref.	Dimensions @ 1 GHz	Operating freq., GHz	Scan angle, deg	Fractional BW, %	Max. gain	Max. efficiency
[18]	$0.5\lambda_0 \times 0.06\lambda_0 \times 0.003\lambda_0$	3.90–4.90	−61 to + 67	22.72	10.5 dBi @ 4 GHz	75% @ 4.25 GHz
[19]	$0.092\lambda_0 \times 0.022\lambda_0 \times 0.003\lambda_0$	13.5–17.8	−57 to + 30	27.47	9 dBi @ 17 GHz	unspecified
[20]	$0.97\lambda_0 \times 0.053\lambda_0 \times 0.009\lambda_0$	57– 63	−25.2 to + 24.6	10.0	23 dBi @ 61 GHz	unspecified
[21]	$0.106\lambda_0 \times 0.083\lambda_0 \times 0.001\lambda_0$	54–60	+ 3 to 12	13.91	11.4 dBi @ 61 GHz	unspecified
[22]	$0.106\lambda_0 \times 0.083\lambda_0 \times 0.001\lambda_0$	16.5–17.2	—	4.2	12 dBi @ 16 GHz	84% @ 14 GHz
This work	$0.062\lambda_0 \times 0.02\lambda_0 \times 0.005\lambda_0$	55–65	−35 to + 34.5	16.66	7.8 dBi @ 62 GHz	84.2% @ 62 GHz

5 References

[1] Henry, R., Okoniewski, M.: ‘A broadside scanning half mode substrate integrated waveguide periodic leaky-wave antenna’, *IEEE Antennas Wirel. Propag. Lett.*, 2014, **13**, (13), pp. 1429–1432

[2] Martínez-Ros, A.J., Gómez-Tornero, J.L., Losada, V.*, et al.*: ‘Non-uniform sinusoidally modulated half-mode leaky-wave lines for near-field focusing pattern synthesis’, *IEEE Trans. Antennas Propag.*, 2015, **63**, (3), pp. 1022–1031

[3] Mahmoud, S.F., Antar, Y.M.M.: ‘Leaky wave antennas: theory and design’. 30th National Radio Science Conf. (NRSC), Cairo, Egypt, April 2013, pp. 1–8

[4] Caloz, C., Itoh, T.: ‘Array factor approach of leaky-wave antennas and application to 1-D/2-D composite right/left-handed (CRLH) structures’, *IEEE Microw. Wirel. Comp. Lett.*, 2004, **14**, (6), pp. 274–276

[5] Lim, S., Caloz, C., Itoh, T.: ‘Electronically scanned composite right/left handed microstrip leaky-wave antenna’, *IEEE Microw. Wirel. Compon. Lett.*, 2004, **14**, (6), pp. 277–279

[6] Siragusa, R., Perret, E., Caloz, C.: ‘A tapered CRLH interdigital/stub leaky-wave antenna with minimized sidelobe levels’, *IEEE Antennas Wirel. Propag. Lett.*, 2012, **11**, pp. 1214–1217

[7] Wu, C.M., Itoh, T.: ‘A wideband/image-rejection distributed mixer integrated with a CRLH leaky wave antenna’. Proc. Asia-Pacific Microw. Conf., Yokohama, Japan, December 2010, pp. 634–637

[8] Alibakhshi-Kenari, M., Naser-Moghadasi, M., Sadeghzadeh, R.A.*, et al.*: ‘Periodic array of complementary artificial magnetic conductor metamaterials-based multiband antennas for broadband wireless transceivers’, *IET Microw. Antennas Propag*, 2016, **10**, (15), pp. 1682–1691

[9] Sievenpiper, D., Zhang, L., Broas, R.F.J.*, et al.*: ‘High-impedance electromagnetic surfaces with a forbidden frequency band’, *IEEE Trans. Microw. Theory Tech.*, 1999, **47**, (11), pp. 2059–2074

[10] Lai, A., Caloz, C., Itoh, T.: ‘Composite right/left-handed transmission line metamaterials’, *IEEE Microw. Mag.*, 2004, **5**, (3), pp. 34–50

[11] Śanchez-Martínez, J.J., Márquez-Segura, E., Otero, P.*, et al.*: ‘Artificial transmission line with left/right-handed behavior based on wire bonded interdigital capacitors’, *Prog. Electromagn. Res. B*, 2009, **11**, pp. 245–264

[12] Caloz, C., Okabe, H., Iwai, T.*, et al.*: ‘Transmission line approach of left-handed metamaterials’. Proc. USNC/URSI National Radio Science Meeting, Boulder, CO, USA, January 2002, **1**, p.39

[13] Lei, L., Caloz, C., Itoh, T.: ‘Dominant mode leaky-wave antenna with backfire-to-endfire scanning capability’, *Electron. Lett.*, 2002, **38**, pp. 1414–1416

[14] Caloz, C., Itoh, T.: ‘Metamaterials for high-frequency electronics’, *Proc. IEEE.*, 2005, **93**, (10), pp. 1744–1752

[15] Jiang, W., Liu, C., Zhang, B.*, et al.*: ‘K-band frequency-scanned leaky-wave antenna based on composite right/left-handed transmission lines’, *IEEE Antennas Wirel. Propag. Lett.*, 2013, **12**, pp. 1133–1136

[16] Sakakibara, K., Ikeda, T., Kikuma, N.*, et al.*: ‘Beam scanning performance of leaky-wave slot array on left-handed waveguide’. IEEE Antennas and Propagation Society Int. Symp., Honolulu, HI, USA, June 2007, pp. 5821–5824

[17] Stutzman, W.L.: ‘Estimating directivity and gain of antennas’, *IEEE Antenn. Propag. M*, 1998, **40**, (4), pp. 7–11

[18] Wu, G.-C., Wang, G.-M., Peng, H.-X.*, et al.*: ‘Design of leaky-wave antenna with wide beam-scanning angle and low cross-polarisation using novel miniaturised composite right/left-handed transmission line’, *IET Microw. Antennas Propag.*, 2016, **10**, (7), pp. 777–783

[19] Zhang, H., Jiao, Y.-C., Zhao, G.*, et al.*: ‘CRLH-SIW-based leaky wave antenna with low cross-polarisation for Ku-band applications’, *Electron. Lett.*, 2017, **52**, (17), pp. 1426–1428

[20] Ma, Z.L., Ng, K.B., Chan, C.H.*, et al.*: ‘A novel supercell-based dielectric grating dual-beam leaky-wave antenna for 60-GHz applications’, *IEEE Trans. Antennas Propag.*, 2016, **64**, (12), pp. 5521–5526

[21] Chang, L., Zhang, Z., Li, Y.*, et al.*: ‘60-GHz air substrate leaky-wave antenna based on MEMS micromachining technology’, *IEEE Trans. Compon. Packag. Manufact. Tech.*, 2016, **6**, (11), pp. 1656–1662

[22] Kianinejad, A., Chen, Z.N., Qiu, C.-W.: ‘A single-layered spoof-plasmon-mode leaky wave antenna with consistent gain’, *IEEE Trans. Antennas Propag*, 2017, **65**, (2), pp. 681–687

[23] Balanis, C. A. ‘*Fundamental parameters of antenna, antenna theory analysis and design*’, (Wiley, Hoboken, NJ, 1997, 2nd edn.), pp. 58–61.

[24] Kharrat, I., Xavier, P., Vuong, T.-P.*, et al.*: ‘Low-loss paper substrate for printed high efficiency antennas at 2.45GHz’, *IEEE Antennas Wirel. Propag. Lett*, 2015, **14**, pp. 1400–1403